

Military Technical College  
Cairo, Egypt



12<sup>th</sup> International Conference  
on Applied Mechanics and  
Mechanical Engineering (AMME)

## INVESTIGATION OF STATIC AND DYNAMIC BEHAVIOR OF PRESSURE COMPENSATED VARIABLE DISPLACEMENT SWASH PLATE AXIAL PISTON PUMP

Tamer A. SALEH\*, M. Galal RABIE\*\*\* and S. E. ABDOU\*\*

### ABSTRACT

This paper is a part of study, conducted to improve the control capabilities of a pressure compensated pump, by implementation of an electrohydraulic controller. This part of was dedicated to investigate the static and dynamic behavior of an axial piston pump of swash plate type. The studied pump is of variable displacement type. It is equipped with a hydromechanical controller (pressure compensator). This controller keeps the pump displacement maximum if the pressure is less than certain limiting value. When the pump exit pressure exceeds this limit, the controller reduces the pump displacement gradually until the real pump flow becomes null. The study starts by deducing detailed mathematical model describing the pump together with its hydromechanical controller. The deduced mathematical model is used to develop a computer simulation program for the studied system using (SIMULINK). The steady state pump flow characteristics were evaluated experimentally and used to validate the simulation results. The comparison of the theoretical and experimental results of the pump flow characteristics showed good agreement between them. The simulation program was used to investigate the dynamic behavior of the pump equipped with its pressure compensator. This class of pump controllers produces unique control law. Any modification of the control law requires major modification of the controller design.

### KEY WORDS

Axial, piston, pump, swash plate, variable displacement, pressure compensator, static, dynamic, transient.

---

\* Graduate student, Dpt. Of Aircraft Mechanics, Egyptian Armed Forces

\*\* Professor, Industrial Engineering Dpt., Modern Academy for Eng. &Tech., Cairo

\*\*\* Ass. Professor, Mechatronics Dpt., Higher Tech. Institute, 10<sup>th</sup> of Ramadan City

**NOMENCLATURE**

$A_{dn}, A_{sn}$	Delivery- suction port area of n <sup>th</sup> pumping chamber, m <sup>2</sup>
$A_p$	Piston area, m <sup>2</sup>
$A_h$	Piston relief hole area, m <sup>2</sup>
$A_{ps1}, A_{ps2}$	Pressure sensor spool projected side areas, m <sup>2</sup>
$A_{sp}$	Servo piston projected area, m <sup>2</sup>
$A_c, A_t$	Valve spool restriction area to controller / to tank line, m <sup>2</sup>
B	Bulk modulus, Pa.
$C_d$	Discharge coefficient.
$C_r$	Swash Plate torque arm, m
$d_p$	Piston diameter, m
$d_{sp}$	Servo piston diameter, m
$F_{psi}$	Servo piston inertia force, N
$F_{nn}$	n <sup>th</sup> piston normal force component, N
$F_{spn}$	Total swash plate force due to n <sup>th</sup> piston, N
$F_{psd}$	Pressure forces affecting the pressure sensor spool, N
$F_{psl}, F_{splr}$	Pressure sensor and servo piston limiter reaction forces, N
$F_{pss}$	Pressure sensor spring force, N
$F_{sps}$	Return spring force, N
$F_{psv}, F_{spv}$	Viscous force, N
$f_{mps}, f_{msp}$	Pressure sensor material damping coefficient, N/(m/s)
$f_r$	Viscous friction coefficient, N/(m/s)
$J_{sw}$	Swash-plate mass moment of inertia, kg · m <sup>2</sup>
$K_{mps}$	Pressure sensor material stiffness, N/m
$K_{ps}$	Pressure sensor spring stiffness, N/m
$K_{msp}$	Servo piston material stiffness, N/m
$K_{sp}$	Servo piston return spring stiffness, N/m
$L_{rn}$	Torque arm length, m
$m_p$	Piston mass, kg
$m_{psr}$	Pressure sensor reduced mass, kg
$m_{adp}$	Pressure sensor spool adaptor mass, kg
$m_{spool}$	Pressure sensor spool mass, kg
$m_{kps}$	Pressure sensor spring mass, kg
$m_{spr}$	Servo piston assembly reduced mass, kg
$m_{ksp}$	Servo piston return spring mass, kg
$m_{spp}$	Servo piston spool mass, kg
$m_{cap}$	Servo return spring cap mass, kg
$P_{dn}$	Piston chamber delivery pressure (n <sup>th</sup> chamber), Pa

$P_{cn}$	Piston chamber pressure, Pa
$P_{sn}$	Piston chamber suction pressure ( $n^{\text{th}}$ chamber), Pa
$P_{sp}$	Pressure applied in servo piston chamber, Pa
$P_d$	Pump load pressure, Pa
$P_t$	Return line pressure, Pa
$Q_{pn}$	Flow rate due to piston displacement, $\text{m}^3/\text{s}$
$Q_{inn}$	Flow rate inlet to the $n^{\text{th}}$ chamber, $\text{m}^3 / \text{s}$
$Q_{outn}$	Flow rate outlet from the $n^{\text{th}}$ chamber, $\text{m}^3 / \text{s}$
$Q_{hn}$	Flow rate through the lubrication hole of $n^{\text{th}}$ piston, $\text{m}^3 / \text{s}$
$Q_c$	Flow rate to the control chamber, $\text{m}^3 / \text{s}$
$Q_t$	Flow rate to the tank line, $\text{m}^3 / \text{s}$
$Q_{Ln}$	$n^{\text{th}}$ piston flow rate, $\text{m}^3 / \text{s}$
$r_{cl}$	Cylinder Pitch Circle radius, m
$R_L$	Leakage resistance, $\text{Pa s}/\text{m}^3$
$R_{psi}, R_{psr}$	Pressure sensor left and right seat reaction forces, N
$T_{\Sigma swp}$	Swash Plate torque, N.m
$T_{swpn}$	Swash plate torque due to $n^{\text{th}}$ piston, N.m
$V_{cn}$	Piston chamber volume, $\text{m}^3$
$V_{ci}$	Piston chamber nominal volume, $\text{m}^3$
$V_{spi}$	Servo piston chamber nominal volume, $\text{m}^3$
$V_{sp}$	Servo piston chamber volume, $\text{m}^3$
$x_{pn}$	$n^{\text{th}}$ Piston displacement, m
$x_{ps}$	Pressure sensor spool displacement, m
$x_{psmax}, x_{spmax}$	Pressure sensor spool and servo piston maximum displacement, m
$x_{ol}, x_{ul}$	Pressure sensor spool–sleeve overlapping and under lapping distance, m
$x_{psi}$	Pressure sensor spring preloading displacement, m
$x_{sp}$	Servo piston displacement, m
$\beta_{sw}$	Swash-plate viscous damping, Nms
$\rho$	Fluid density, $\text{kg}/\text{m}^3$
$\alpha_{loc}$	Local swash plate angle, rad
$\theta_n$	$n^{\text{th}}$ Piston angular position, rad
	Angular speed of cylinder block, rad/s
$\alpha$	Swash plate angle, rad

## 1. INTRODUCTION

Variable displacement axial piston pumps are widely used in different engineering fields. They are equipped with controllers, producing wide range of control laws. The pressure compensators are among the most widely used controllers. This class of controller forces the pump to operate at its maximum displacement volume if the pressure is less than certain pre-set value. If the load pressure exceeds this value, the controller starts to reduce the pump displacement progressively until it reaches its minimum value. Then, the pump delivers minimum flow rate, just equal to the pump leakage flow. The real pump flow then becomes null.

Conventionally, the pressure compensator consists of two basic elements, a pressure sensor and a servo piston. These elements are pure hydromechanical elements. Actually, the controller of this class produces certain, fixed, control law, while the electrohydraulic servo-controllers (EHSC) are capable to produce wide range of control laws. Therefore the authors conducted a study to explore the capability of EHSC in producing different control laws, for the studied pump.

This paper contains the first part of this study. It deals with the modeling and simulation of a pressure compensated axial piston pump of swash plate type. This class of pump received more interest in the last two decades. Most of them were directed to the dynamics of pump controllers, while few papers were dedicated to the analysis of behavior of pumping mechanism itself. The works of Schoeneu (1990), Rabie (1990), Manring (1996), Zhang (2001) and Alshammari (2004), were among the most interesting and fruitful studies of this subject.

## 2. DESCRIPTION OF THE STUDIED PUMP

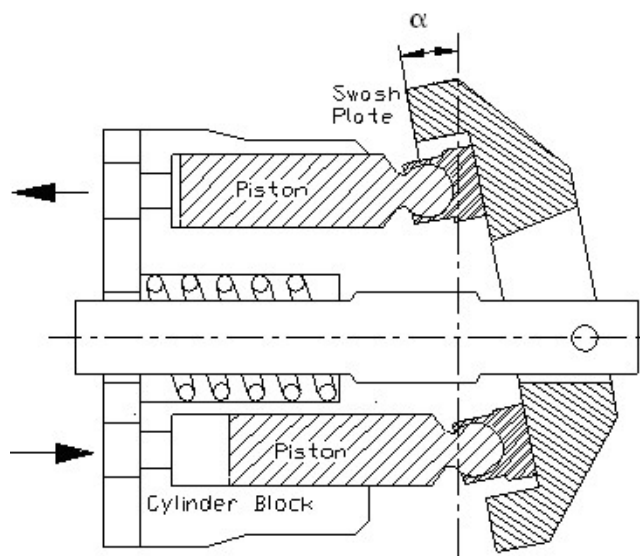


Fig.1 Scheme of the pumping mechanism of a swash plate axial piston pump

The studied pump is a variable displacement axial piston pump of swash plate type, Fig.1. The pump displacement is controlled by a pressure compensator. The pump controller consists of a pressure sensor and a servo piston, while the pumping mechanism consists of the following elements, Figs. 1&2:

- Pistons-slipper pads assembly(9 of them).
- Rotating cylinder block.
- Port plate assembly.
- Swash-plate assembly.
- Drive shaft assembly.

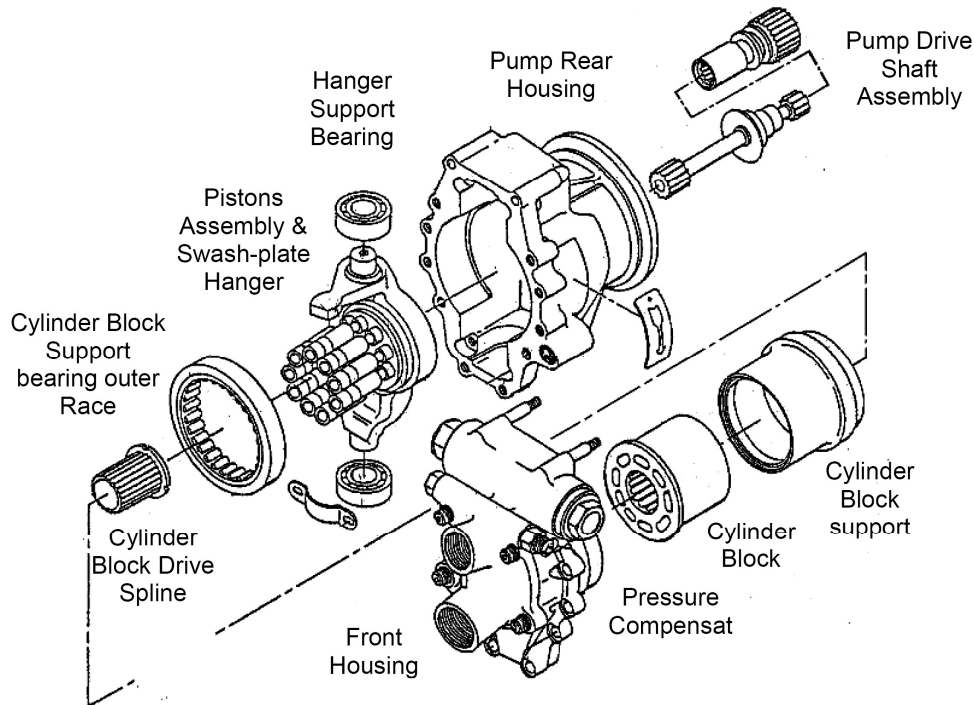


Fig.2. Exploded view of the studied pump

### 3. MATHEMATICAL MODEL OF THE PUMP

**Continuity equation applied to the piston chamber:**

The following is the continuity equation applied to the n<sup>th</sup> piston chamber, Fig.1.

$$\frac{V_{cn}}{B} \left( \frac{dP_{cn}}{dt} \right) = [Q_{pn} + Q_{inn} - Q_{outn} + Q_{hn} - Q_{Ln}]$$

Or 
$$\frac{dP_{cn}}{dt} = \frac{B}{V_{cn}} [Q_{pn} + Q_{inn} - Q_{outn} + Q_{hn} - Q_{Ln}] \quad (1)$$

The volume of the piston chamber changes with the piston displacement.

$$V_{cn} = V_{ci} - A_p \cdot x_{pn} \quad (2)$$

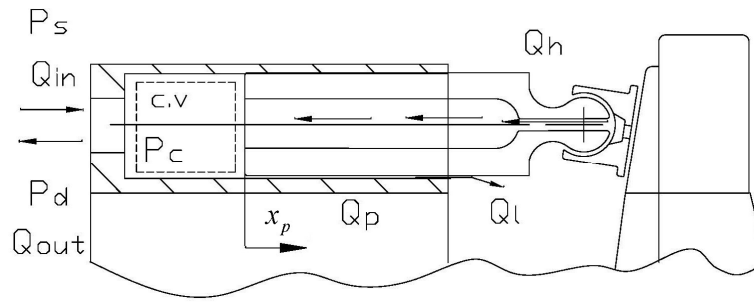


Fig.3. Flow rates inlet to and outlet from piston chamber

Flow Rate outlet from the n piston chamber  $Q_{out}$ :

$$Q_{outn} = C_{do} \cdot A_{dn}(\theta_n) \sqrt{\frac{2}{\rho} (P_{cn} - P_d)} \text{sign}(P_{cn} - P_d) \tag{3}$$

Flow Rate  $Q_{in}$  :

$$Q_{inn} = C_{di} \cdot A_{sn}(\theta_n) \sqrt{\frac{2}{\rho} (P_s - P_{cn})} \text{sign}(P_s - P_{cn}) \tag{4}$$

The use of constant discharge flow coefficients of value (0.7) for computational reason is convenient.

The leakage flow rate  $Q_{Ln}$ :

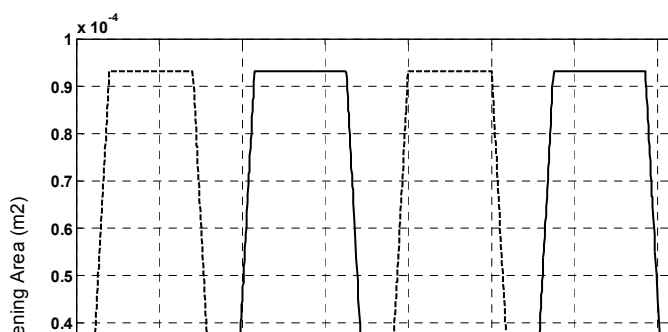
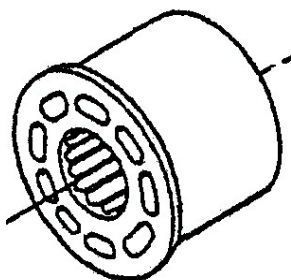
The internal leakage flow is assumed to be laminar and occurs at low Reynolds number [9]. It is considered to vary linearly and proportional to the pressure build up [7], so it follows the following equation:

$$Q_{Ln} = P_{cn} / R_L \tag{5}$$

The resistance to leakage  $R_L$  is determined experimentally.

**Port plate effective areas (Ad and As):**

The hydraulic oil flows into, and out of, the piston chamber through the port plate, Fig.4. It contains two crescent shaped openings which intersect with the opening holes of piston chambers. This intersection creates throttling areas communicating the piston chamber with the inlet and delivery ports ( $A_s$  &  $A_d$  respectively). The variation of these areas with the angular position ( $\theta_n$ ) of the considered piston chamber was calculated and plotted in Fig.4.





The relief hole flow rate  $Q_{hn}$  :

An additional amount of flow enters and exits from the piston chamber through a tiny relief hole Fig.5. This hole is drilled through the piston head, ball and socket side. This flow lubricates the contact area between the slipper-pad and swash plate. It is described by the following equation.

$$Q_{hn} = C_{dh} \cdot A_h \sqrt{\frac{2}{\rho} (P_{cn} - P_t) \text{sign}(P_{cn} - P_t)} \quad (6)$$



Fig.5

Piston Kinematics:

The values of pistons displacement, speed and acceleration are needed to calculate the flow rates, pressures and forces. Figure 6 shows the position of the piston, relative to the swash plate, for certain rotational angle. The piston kinematics is described by the following equations.

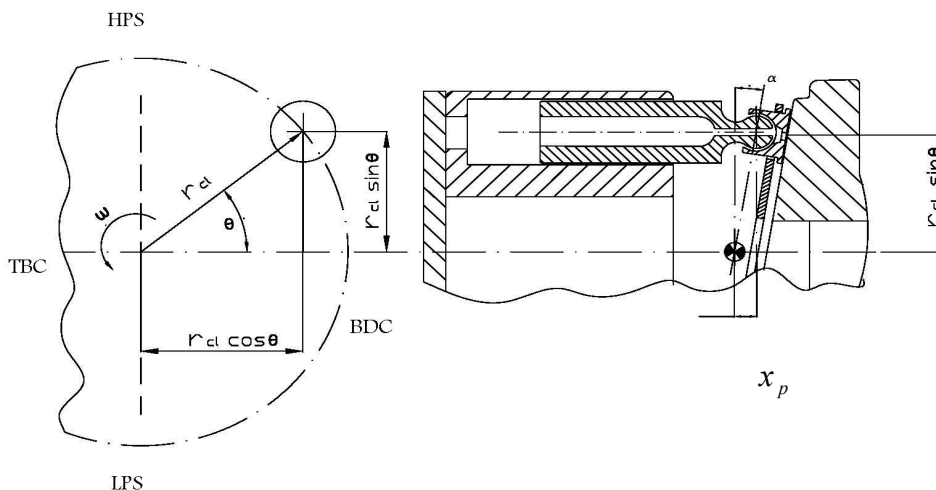


Fig.6 Piston motion mathematical analysis

• Piston Displacement:

$$x_{pn} = r_{cl} \sin \theta_n \cdot \tan \alpha + r_{cl} \cdot \tan \alpha_{loc} \quad (7)$$

Where, for a 9-piston pump;  $\theta_n = \int \omega dt + \frac{2\pi}{9} n$  (8)

• Piston Velocity:

$$\dot{x}_{pn} = r_{cl} \omega \cos \theta_n \tan \alpha + r_{cl} \sin \theta_n (1 + \tan^2 \alpha) \dot{\alpha}$$
 (9)

For fixed displacement pump, the swash plate angle  $\alpha$  is constant, then;

$$\dot{x}_{pn} = r_{cl} \omega \cos \theta_n \tan \alpha$$
 (9a)

• Piston Acceleration:

$$\ddot{x}_{pn} = r_{cl} \omega \cdot \cos \theta_n \cdot (1 + \tan^2 \alpha) \ddot{\alpha} - r_{cl} \omega^2 \sin \theta_n \tan \alpha$$
 (10)

For fixed displacement pump;

$$\ddot{x}_{pn} = -r_{cl} \omega^2 \sin \theta_n \tan \alpha$$
 (10a)

■ Piston forces

The piston motion is affected by the pressure, inertia and viscous friction forces. The following is the equation of motion of piston subjected to these forces.

$$P_{cn} A_p = m_p \ddot{x}_{pn} + f_p \dot{x}_{pn} + F_{SPn}$$
 (11)

Thus, the following expression could be deduced for the swash plate force, due to the action of the nth piston;  $F_{SPn}$ .

$$F_{SPn} = \frac{\pi}{4} P_{cn} d_p^2 + m_p \omega^2 r_{cl} \sin \theta_n \tan \alpha$$
 (12)

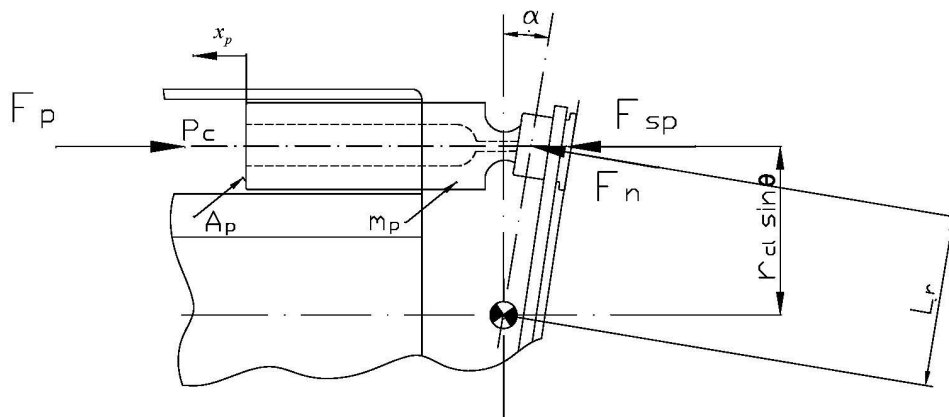


Fig.7 Forces affecting single piston

The total instantaneous torque acting on the swash plate consists of two main components. The major component is the reaction to the pressure force acting on pistons, while the second component is the force due to the pistons inertia forces. The, neglecting the inertia of oil column filling the pumping chamber, the swash plate torque can be deduced as follows.

The torque arm  $L_m$  is given by:

$$L_m = r_{cl} \frac{\sin \theta_n}{\cos \alpha} \tag{13}$$

Considering the directions of forces and dimensions, illustrated by Fig. 7, the following expressions for piston force and corresponding swash plate torque were deduced.

$$F_{nn} = \frac{F_{spn}}{\cos \alpha} \tag{14}$$

$$T_{swpn} = F_{nn} L_m \tag{15}$$

$$T_{swpn} = \frac{F_{spn}}{\cos \alpha} \cdot \left( r_{cl} \frac{\sin \theta_n}{\cos \alpha} \right) \tag{16}$$

$$T_{swpn} = \left( P_{cn} \cdot \frac{\pi}{4} d_p^2 + m_p r_{cl} \omega_n^2 \cdot \sin \theta_n \cdot \tan \alpha \right) \cdot r_{cl} \frac{\sin \theta_n}{(\cos \alpha)^2} \tag{17}$$

#### 4. PRESSURE COMPENSATOR MATHEMATICAL MODEL

The pressure compensator consists of two elements, a pressure sensing element and a servo piston. The servo piston drives the swash plate. For certain range of pump exit pressure, the servopiston displacement, and the swash plate angle, are proportional to the pressure sensor displacement. The equations describing the pressure compensator are given in the following.

##### • Pressure Sensor equation of motion

Figure 8 shows the valve spool free body diagram. It illustrates the different forces affecting the spool. The motion of the spool and attached parts are governed by the following equation of motion:

$$F_{psi} + F_{pss} + F_{psv} = F_{psl} + F_{psd}$$

Or 
$$m_{psr} \ddot{x}_{ps} + k_{ps} (x_{psi} + x_{ps}) + f_r \dot{x}_{ps} + P_t A_{ps2} = F_{psl} + P_d A_{ps1} \tag{18}$$

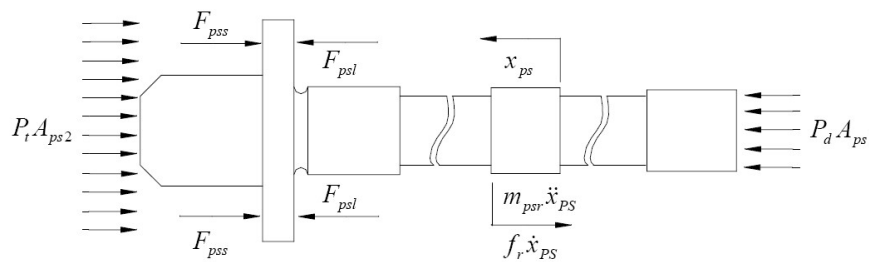


Fig. 8 Pressure sensor spool free body diagram

where 
$$m_{psr} = m_{spool} + m_{adp} + \frac{1}{2} m_{kps} \tag{19}$$

The pressure sensor displacement is limited by single side mechanical stop. This limiter reaction force could be described as a material stiffness ( $K_{mps}$ ) and material damping coefficient ( $f_{mps}$ ). Actually, the spool is positioned at far right against the

right seat, under the action of the spring force. The seat reaction force will follow the conditional equation:

$$\left. \begin{aligned} R_{psr} &= K_{mps} |x_{ps}| + f_{mps} \dot{x}_{ps} & x_{ps} < 0 \\ R_{psr} &= 0 & x_{ps} \geq 0 \end{aligned} \right\} \quad (20)$$

### Servo-Actuator force Analysis

Figure 9 illustrates the stroking piston free body diagram. The Actuating piston and the attached parts of motion are governed by the following equation of motion.

$$\begin{aligned} m_{spr} \ddot{x}_{sp} + k_{sp} (x_{spi} + x_{sp}) + f_r \dot{x}_{sp} + (T_{\Sigma swp} / C_r) \\ = F_{psl} + (P_{sp} - P_t) A_{sp} \end{aligned} \quad (21)$$

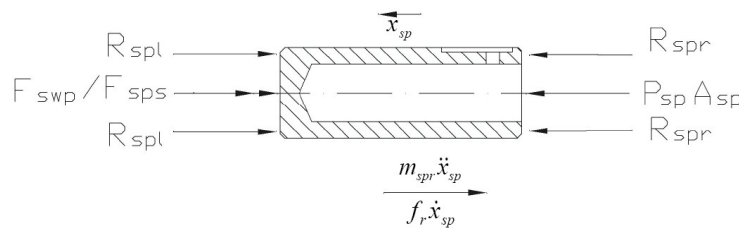


Fig. 7 Forces affecting the servo piston

where  $m_{spr} = m_{spp} + m_{cap} + 0.5m_{ksp} \ddot{x}_{sp}$  (22)

- Limiter reaction forces.

The servo piston displacement is limited by two mechanical stops. The seat reaction force could be described as a material stiffness ( $K_{msp}$ ) and material damping coefficient ( $f_{msp}$ ). The reaction force will follow this conditional relation:

$$\left. \begin{aligned} R_{spr} &= K_{msp} |x_{sp}| + f_{msp} \dot{x}_{sp} & \text{for } x_{sp} < 0 \\ R_{spr} &= 0 & \text{for } x_{sp} \geq 0 \end{aligned} \right\} \quad (23)$$

As the servo piston travels to the left, and reaches the travel end it will be positioned against the left seat, by this time the reaction force will follow this conditional equation:

$$\left. \begin{aligned} R_{spl} &= 0 & \text{for } x_{sp} < x_{spmax} \\ R_{spl} &= K_{msp} (x_{sp} - x_{spmax}) + f_{msp} \dot{x}_{ps} & \text{for } x_{sp} \geq x_{spmax} \end{aligned} \right\} \quad (24)$$

- Swash Plate force.

$$F_{swp} = T_{\Sigma swp} / C_r \quad (25)$$

The swash-plate rotational motion is considered by introducing the mass moment of inertia effect as follows:



$$Q_c = C_d A_c (x_{ps}) \sqrt{\frac{2}{\rho} (|P_d - P_{sp}|)} \text{sign}(P_d - P_{sp}) \quad (28)$$

To Tank flow rate  $Q_t$

$$Q_t = C_d A_t (x_{ps}) \sqrt{\frac{2}{\rho} (|P_{sp} - P_t|)} \text{sign}(P_{sp} - P_t) \quad (29)$$

The servopiston internal leakage changes linearly with the applied pressure

$$Q_L = P_{sp} / R_L \quad (30)$$

The servo piston chamber volume is related to the piston position, and the nominal chamber volume.

$$V_{sp}(x_{ps}) = V_{spi} + A_{sp} x_{ps} \quad (31)$$

The pressure sensor spool land controls the flow direction Fig.11 It controls two restriction areas,  $A_c$  and  $A_t$ . The restrictor  $A_c$  permits the flow to go from the sensing chamber to the controller servo piston. On the other hand, the restrictor  $A_t$  permits the flow to go from the servo piston chamber to the case drain / tank line.

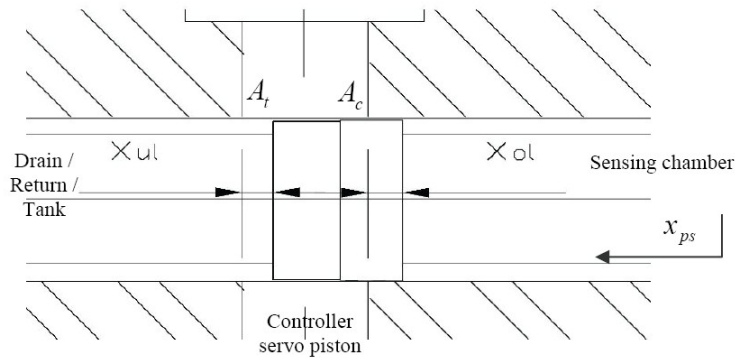


Fig.11 pressure sensor spool land

The restriction area ( $A_c$ ) is divided into two margins, clearance and sector areas.

$$\left. \begin{aligned} A_c(x_{ps}) &= b_{c1} \times t_{c1} & \text{for } 0 \leq x_{ps} < x_{ol} \\ A_c(x_{ps}) &= \frac{x_{ps}}{6S_1} [3x_{ps}^2 + 4S_1^2] & \text{for } x_{ol} \leq x_{ps} < x_{psmax} \end{aligned} \right\} \quad (32)$$

The restriction area ( $A_t$ ) is divided into two margins, sector and clearance areas.

$$\left. \begin{aligned} A_t(x_{ps}) &= \frac{x_{ps}}{6S_2} [3x_{ps}^2 + 4S_2^2] & \text{for } 0 \leq x_{ps} < x_{ul} \\ A_t(x_{ps}) &= b_{t2} \times t_{t2} & \text{for } (x_{ul} \leq x_{ps} < x_{psmax}) \end{aligned} \right\} \quad (33)$$

The pressure compensated pump is described mathematically by equations (1 to 33). The deduced mathematical model was used to develop a computer simulation program, using the SIMULINK program.

#### **4. EXPERIMENTAL WORK AND MODEL VALIDATION**

The pump static flow-pressure characteristics were measured for different pump speeds (2000, 2500 and 3000 rpm). A variable area throttle valve (loading orifice) was used to generate a pump loading pressure. Figure 12 shows the hydraulic circuit of the test stand.

The validity of pump simulation program is checked by comparing experimental and theoretical results, Fig.13. This figure shows the steady state flow characteristics of the pressure compensated pump for different pump speeds (200, 2500 & 5000 rpm). The experimental and theoretical results are in good agreement between, which validates the simulation program in the steady state.

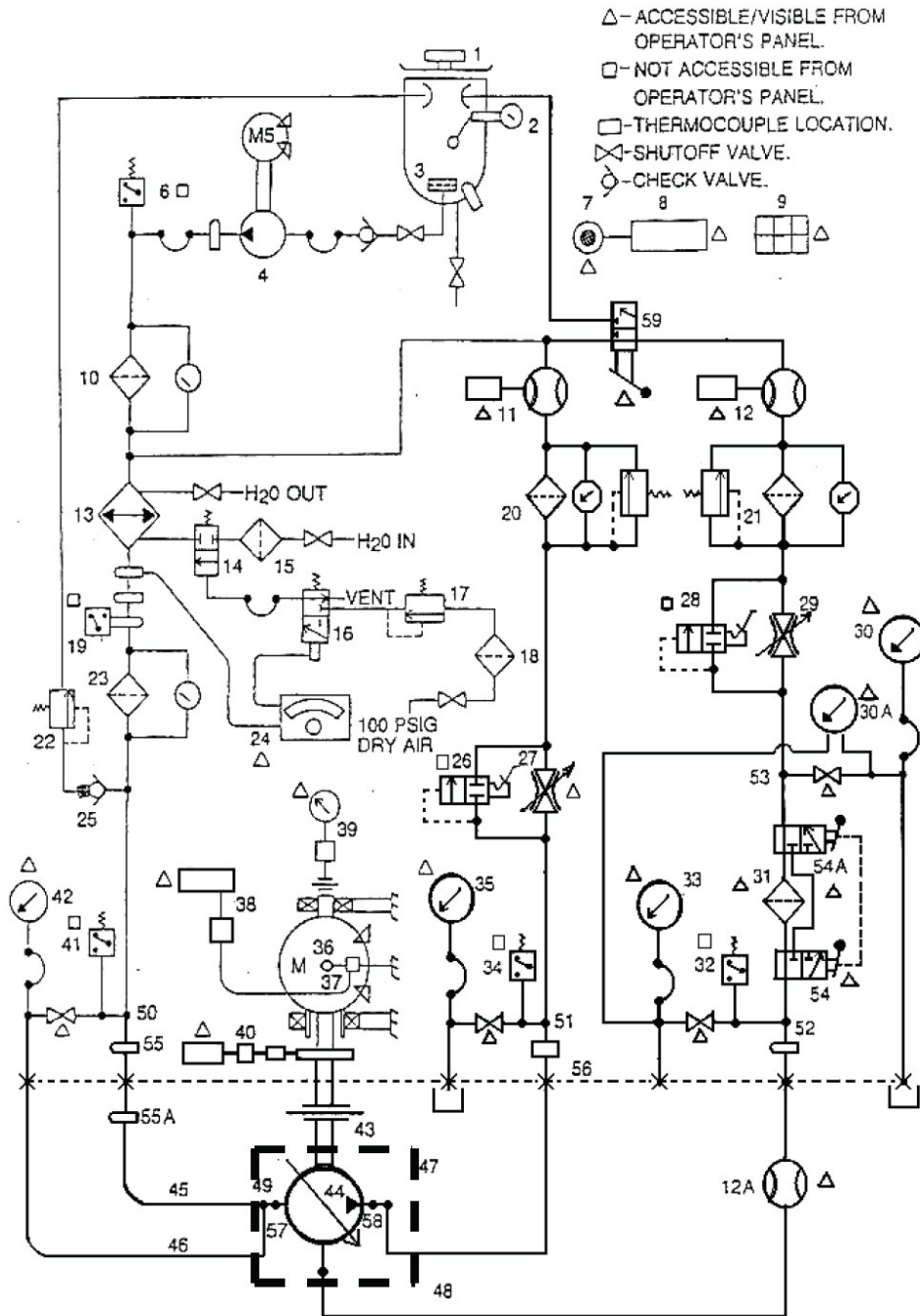


Fig.12 Hydraulic circuit of the pump test stand

The transient response of the lump was evaluated theoretically by using the simulation program. A throttle valve was installed at the pump outlet to control the pump exit pressure. The transient response of the pump to step decrease of the throttle valve area was calculated for different pump speeds (1500, 2000, 2500, 3000, 3500, 4000, 4500 and 5000 rpm). The throttle area variation was calculated to produce an increase in the steady state exit pressure in the range:

- from 3.5 to 206 bars, Fig.14,
- from 3.5 to 208 bars, Fig.15,
- from 3.5 to 210 bars, Fig.16.

The basic features of the transient response (maximum percentage overshoot and settling time) are illustrated in Figs. 17& 18.

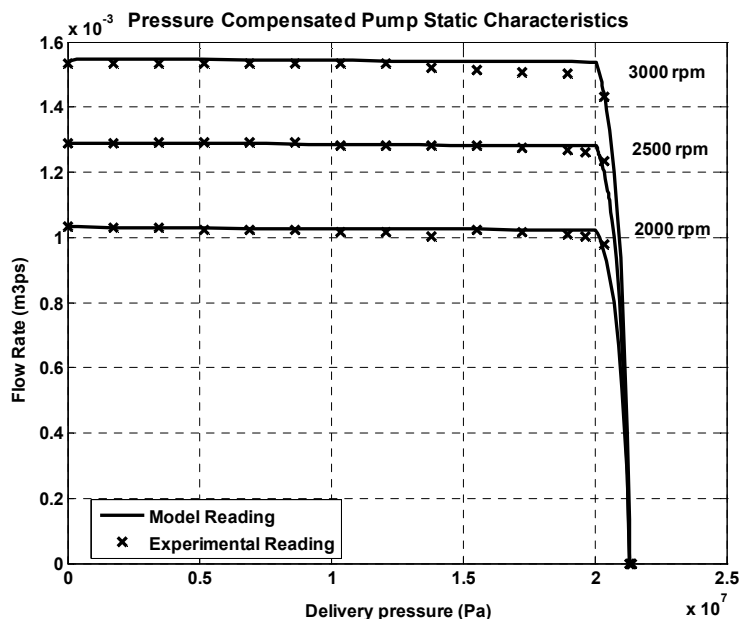


Fig.13 Experimental and theoretical static characteristics of pump

Figure 17 shows that the variations of the maximum percentage overshoot with the pump speed and the size of the applied step. Generally, the responses overshoot increases with the increase in pump speed. This increase is too slight for small sizes of step input, while it becomes more important as the step size approaches the maximum pressure, determined by the compensator setting.

The settling time decreases with the increase in pump speed, Fig.18. The reduction of the settling time reaches up to 50% of its original value as the speed increases from 1500 to 5000 rpm.

## 5. CONCLUSION

This part of was dedicated to investigate the static and dynamic behavior of a variable displacement axial piston pump of swash plate type. The studied pump is equipped with a hydromechanical controller (pressure compensator). The study starts by deducing detailed mathematical model describing the pump together with its hydromechanical controller. The deduced mathematical model was used to develop a computer simulation program for the studied system.

The steady state pump flow characteristics were evaluated experimentally. The simulation and experimental results showed good agreement, which validates the simulation program in the steady state operating modes.

The simulation program was used to investigate the transient response of the pressure compensated pump. The analysis of results showed that the pump is stable in the whole range of operating pressure and speed. The maximum percentage overshoot and settling time are considerably affected by the pump speed and size of applied step. This result should be considered when using this class of pumps in systems including fast response elements such as the hydraulic and electrohydraulic servos.

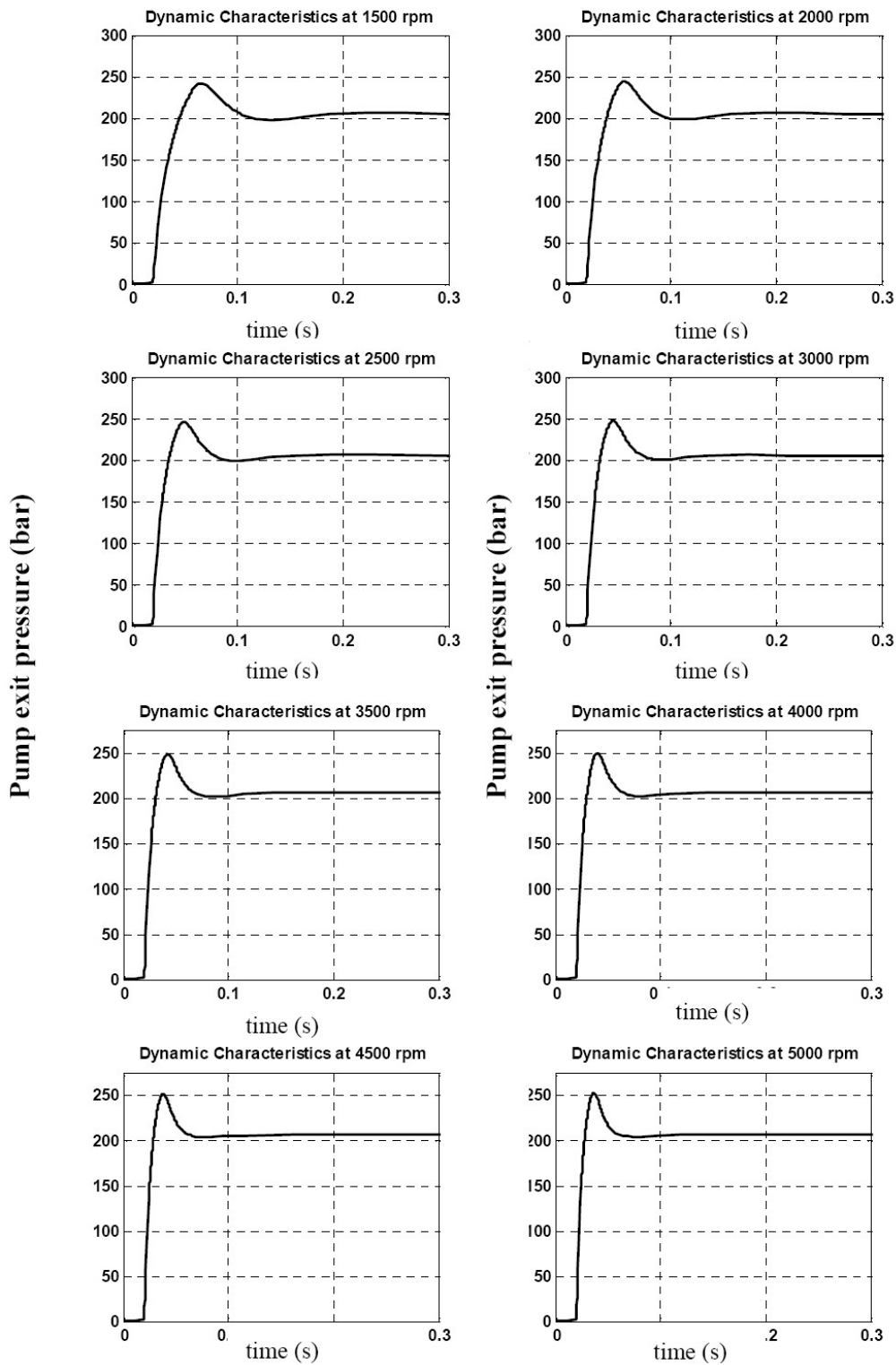


Fig.14 Pump exit pressure transient response due sudden loading pressure increase (from 3.5 to 206 bar)

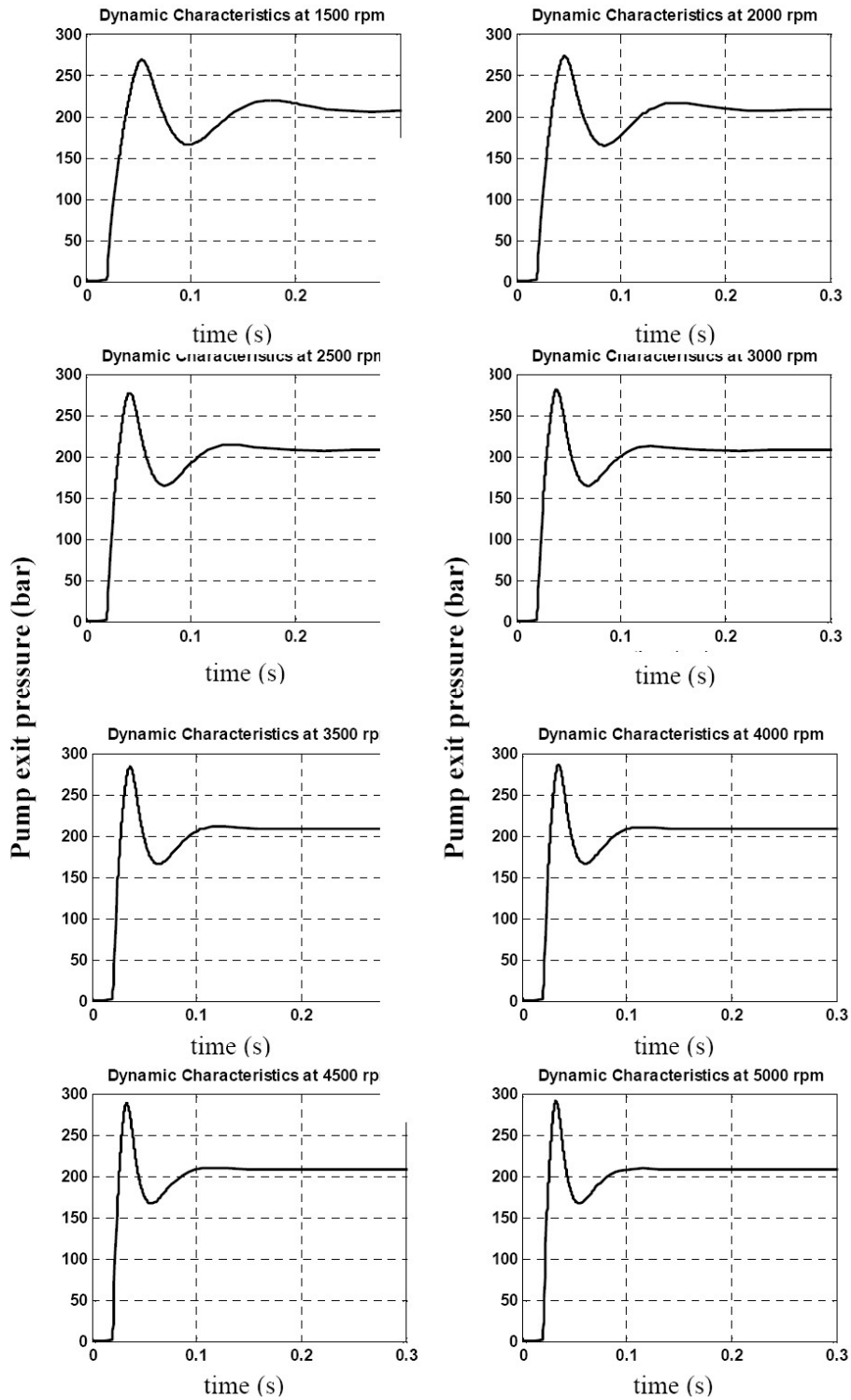


Fig.15 Pump exit pressure transient response due sudden loading pressure increase (from 3.5 to 208 bar)

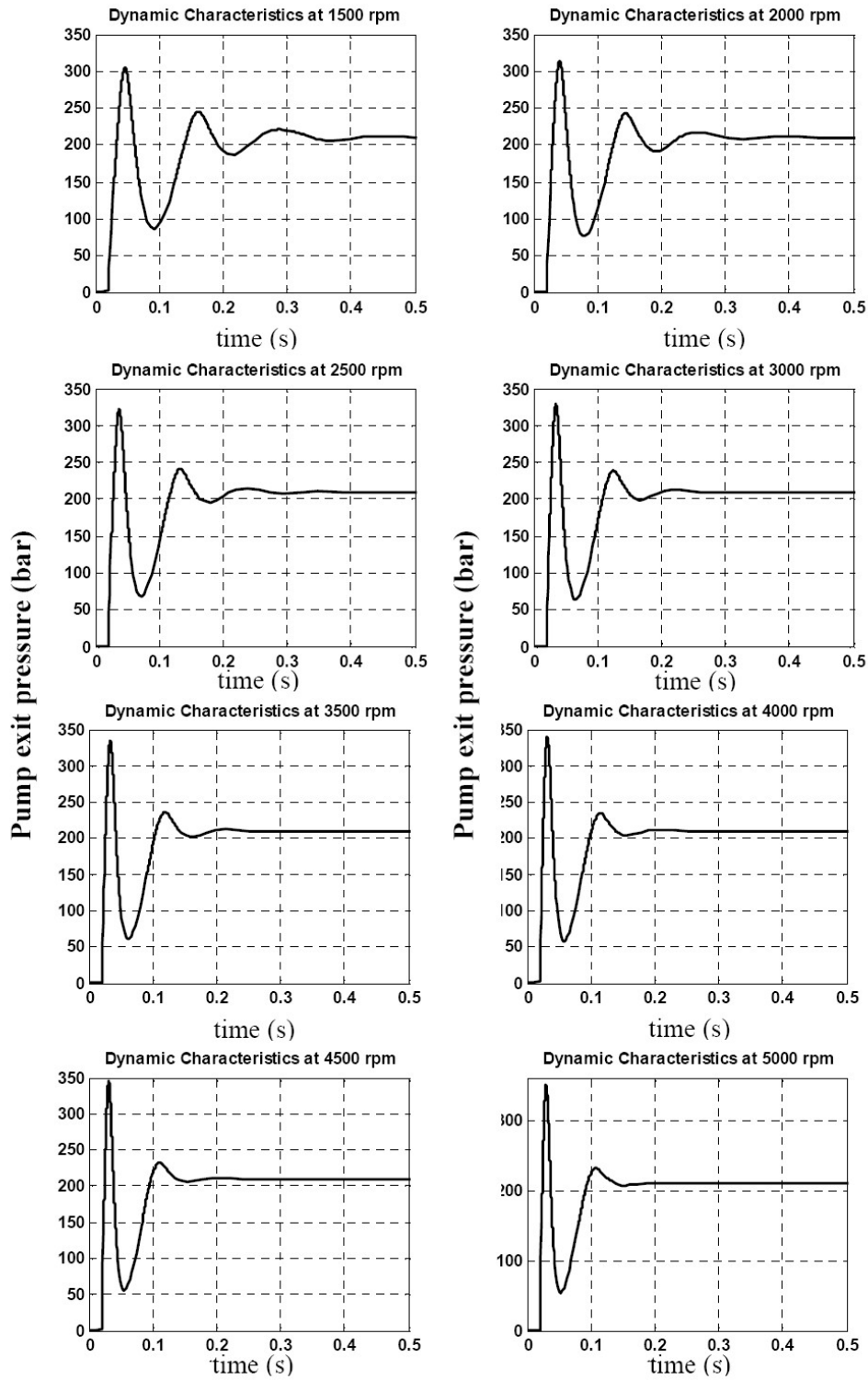


Fig.16 Pump exit pressure transient response due sudden loading pressure increase (from 3.5 to 210 bar)

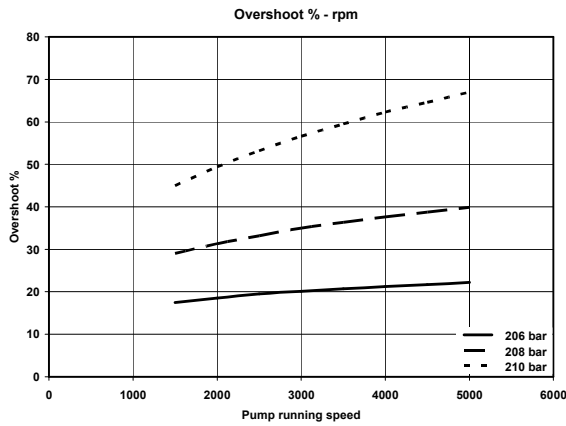


Fig.17 Variation of the maximum percentage overshoot with the pump speed for different step sizes

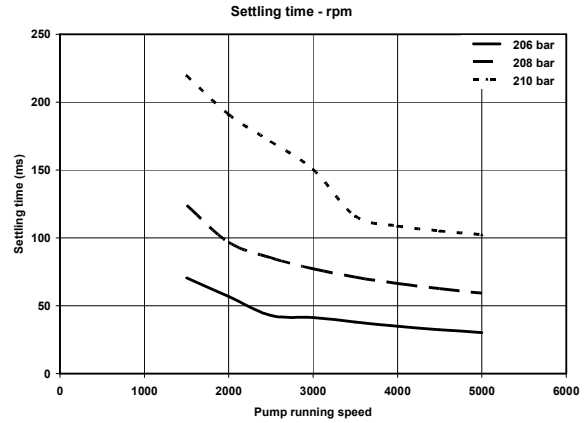


Fig.18 Variation of the settling time with the pump speed for different step sizes

**REFERENCES**

- [1] G. J. Schoeneu, R. T. Burton and G. P. Kavanagh “Dynamic Analysis of a Variable Displacement Pump”, Journal of Dynamic Systems, Measurement and Control, transaction of the ASME, March 1990, vol. 112.
- [2] M. G. Rabie and I. Saleh, “On the Dynamics of Pressure Compensated Variable Geometric Volume Axial Piston Pump” , transaction of Hellwan University, Vol. 6- December 1990
- [3] N. D. Manring and R. E. Johnson. “Modeling and designing a variable-displacement open-loop pump”, Journal of Dynamic Systems, Measurement and Control, transaction of the ASME June 1996 Vol.118
- [4] X. Zhang, J. Cho, S. S. Nair and N. D. Manring, ” New swash plate damping model for hydraulic axial piston pump”, Journal of Dynamic Systems, Meas. and Control, transaction of the ASME, September 2001, vol. 123
- [5] Awadh T. Alshammari, An Investigation into different types of controllers of variable displacement axial piston pumps, PhD thesis, University of West of England-UWE-Bristol,2004